Experimental Petrology of the 1991-1995 Unzen Dacite, Japan. Part I: Phase Relations, Phase Composition and Pre-eruptive Conditions

Francois, Holtz
Sato, Hiroaki
Jared, Lewis
Herald, Behrens
Nakada, Setsuya

(Citation)
Journal of Petrology,46(2):319-337

(Issue Date)
2005

(Resource Type)
journal article

(Version)
Version of Record

(URL)
https://hdl.handle.net/20.500.14094/90001064

JOURNAL OF PETROLOGY | VOLUME 46 | NUMBER 2 | PAGES 319–337 | 2005 | doi:10.1093/petrology/egh077

Experimental Petrology of the 1991–1995 Unzen Dacite, Japan. Part I: Phase Relations, Phase Composition and Pre-eruptive Conditions

FRANCOIS HOLTZ[1]*, HIROAKI SATO[2], JARED LEWIS[1]†, HARALD BEHRENS[1] AND SETSUYA NAKADA[3]

[1]INSTITUTE FOR MINERALOGY, UNIVERSITY OF HANNOVER, WELFENGARTEN 1, D-30167 HANNOVER, GERMANY

[2]DEPARTMENT OF EARTH AND PLANETARY SCIENCES, FACULTY OF SCIENCE AND GRADUATE SCHOOL OF SCIENCE AND TECHNOLOGY, KOBE UNIVERSITY, KOBE, 657-8501 JAPAN

[3]EARTHQUAKE RESEARCH INSTITUTE, UNIVERSITY OF TOKYO, YAYOI 1-1-1, BUNKYO, TOKYO, 113-0032 JAPAN

RECEIVED NOVEMBER 10, 2002; ACCEPTED SEPTEMBER 7, 2004
ADVANCE ACCESS PUBLICATION OCTOBER 28, 2004

Crystallization experiments were conducted on dry glasses from the Unzen 1992 dacite at 100–300 MPa, 775–875°C, various water activities, and fO_2 *buffered by the Ni–NiO buffer. The compositions of the experimental products and natural phases are used to constrain the temperature and water contents of the low-temperature and high-temperature magmas prior to the magma mixing event leading to the 1991–1995 eruption. A temperature of 1050 ± 75°C is determined for the high-temperature magma based on two-pyroxene thermometry. The investigation of glass inclusions suggests that the water content of the rhyolitic low-temperature magma could be as high as 8 wt %* H_2O*. The phase relations at 300 MPa and in the temperature range 870–900°C, which are conditions assumed to be representative of the main magma chamber after mixing, show that the main phenocrysts (orthopyroxene, plagioclase, hornblende) coexist only at reduced water activity; the water content of the post-mixing dacitic melt is estimated to be 6 ± 1 wt %* H_2O*. Quartz and biotite, also present as phenocrysts in the dacite, are observed only at low temperature (below 800–775°C). It is concluded that the erupted dacitic magma resulted from the mixing of* c. *35 wt % of an almost aphyric pyroxene-bearing andesitic magma (1050 ± 75°C; 4 ± 1 wt %* H_2O *in the melt) with 65 wt % of a phenocryst-rich low-temperature magma (760–780°C) in which the melt phase was rhyolitic, containing up to 8 ± 1 wt %* H_2O*. The proportions of rhyolitic melt and phenocrysts in the low-temperature magma are estimated to be 65% and 35%, respectively. It is emphasized that the strong variations of phenocryst compositions, especially plagioclase, can be explained only if there were variations of temperature and/or water activity (in time and/or space) in the low-temperature magma.*

KEY WORDS: *Unzen volcano; magma mixing; experimental study*

INTRODUCTION

Experimental phase equilibria investigations of the ejecta of recent volcanic eruptions are tools to elucidate the physical conditions of crystallization of phenocryst minerals in magma chambers, as shown in several studies (e.g. 1980 Mount St. Helens eruption, Rutherford *et al.*, 1985; 1982 El Chichón eruption, Luhr *et al.*, 1990; 1995–1997 Soufrière Hills eruption, Barclay *et al.*, 1998; 1902 eruption of Mt. Pelée, Martel *et al.*, 1999; 1991 Pinatubo eruption, Scaillet & Evans, 1999). In the case of Unzen volcano, SW Japan, Sato *et al.* (1999) and Venezky & Rutherford (1999) investigated phase equilibria in the range 40–200 MPa from samples of the 1991–1995 dome growth eruptions. However, the experiments were mainly performed to constrain the stability field of hornblende. They were conducted at water-saturated conditions only, and the chemical composition of the experimentally synthesized phases was not reported (Venezky & Rutherford, 1999). The present study is

*Corresponding author. E-mail: f.holtz@mineralogie.uni-hannover.de
†Present address: Department of Earth Science, Rice University, Houston, TX 77251-1892, USA.

undertaken to constrain the pre-eruptive conditions integrating new results from (1) phase equilibrium studies of the 1992 dacite and (2) the investigation of the composition of minerals. The experimental data are compared with the natural rocks (both for the phenocryst assemblage and the phase chemistry) to infer the magmatic conditions and processes in the magma chamber of the 1991–1995 Unzen eruption.

PETROGRAPHY OF THE 1991–1995 DACITE AND A MAGMA MIXING MODEL

Magmas involved in the Unzen eruption

Previous studies (e.g. Nakada & Fujii, 1993; Nakamura, 1995; Nakada & Motomura, 1999; Venezky & Rutherford, 1999) have shown that magma mixing between a phenocryst-rich low-temperature magma and a nearly aphyric high-temperature magma took place before the eruption of the 1991–1995 dacite. This is based on petrographic evidence in the dacite such as reverse zoning of the outer rims of hornblende, plagioclase and magnetite (increase of mole % Usp from 17 to 23% from the core to the rim; Nakamura, 1995), embayed quartz and biotite phenocrysts, and reaction rims of pargasitic hornblende surrounding biotite phenocrysts. These studies concluded that most of the phenocryst minerals belonged to the low-temperature end-member magma, and their equilibration temperature was estimated to be *c.* 780–800°C from the core compositions of iron–titanium oxide phenocrysts (Venezky & Rutherford, 1999). Post-mixing temperatures were estimated to be 900 ± 30°C by those workers. However, to be able to better model the processes in the Unzen magma chamber prior to and after mixing, the temperature and composition of the nearly aphyric high-temperature magma, as well as the bulk composition and melt composition of the low-temperature magma, need to be better constrained. In the following section, we discuss the results of chemical analyses of the phenocrysts and melt inclusions and present an improved model of magma mixing for the 1991–1995 dacite of Unzen volcano. The petrological constraints combined with experimental data are then used to interpret the crystallization conditions of phenocryst minerals in the mixed dacite.

Petrography of the 1991–1995 dacite

Phenocryst phases in the dacite include plagioclase, quartz, hornblende, biotite, clinopyroxene (cpx), orthopyroxene (opx), magnetite, ilmenite, and apatite. Plagioclases are the largest (in size) and most abundant phenocrysts (most grains are in the size range 0·5–1 cm; 15–20 vol. %). Cpx is the least abundant phase (excluding the accessory phases magnetite, ilmenite, apatite) and is difficult to distinguish macroscopically. The modal proportion of all the phenocrysts is *c.* 20–30 vol. % (Nakada & Motomura, 1999). Figure 1 shows histograms of the Mg-number [Mg-number = 100 × Mg/(Mg + Fe)] of mafic phenocrysts and the An content of plagioclase phenocrysts in the 1991–1995 dacite. Opx phenocrysts have a bimodal distribution compositionally. The Mg-number of the groundmass opx is between the Mg-number of the two populations of opx phenocrysts, suggesting that the groundmass opx crystallized from an intermediate melt composition resulting from the mixing of two opx-bearing magmas. The Cr_2O_3 content of the high Mg-number opx and cpx is in the range 0·2–0·5 wt %. Chromium is a compatible element and its concentration decreases rapidly as crystallization proceeds. Therefore, the high Cr_2O_3 content of the high Mg-number

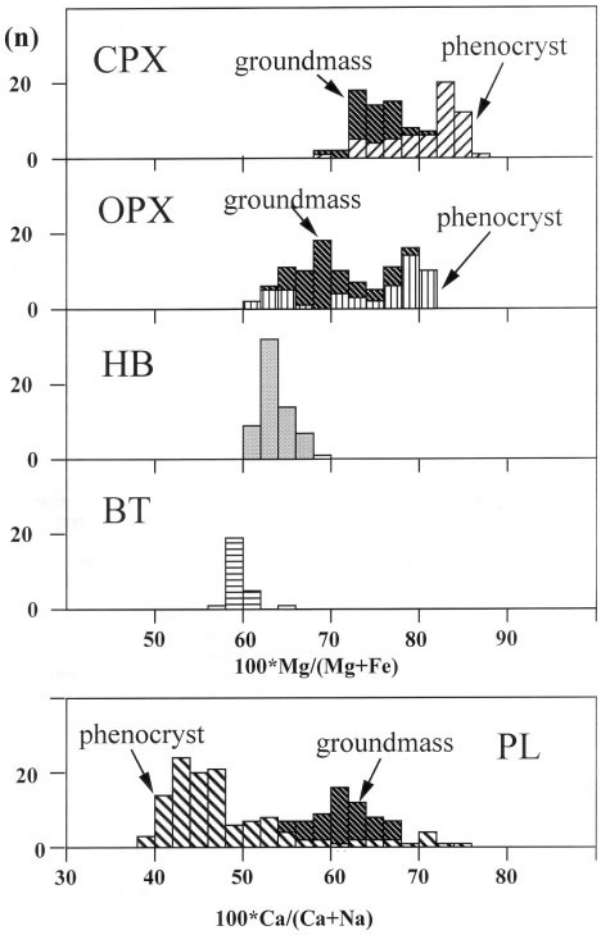

Fig. 1. Mg-number [100 × Mg/(Mg + Fe)] of mafic phenocrysts and An content [100 × Ca/(Ca + Na)] of plagioclase phenocrysts in the 1991–1995 dacites of Unzen volcano. The bimodal distribution of orthopyroxene phenocrysts should be noted (*n* is the number of analyses). The compositions of orthopyroxenes, clinopyroxenes and plagioclases from the groundmass are also plotted.

pyroxenes suggests that they crystallized from a relatively primitive magma and that these minerals could compose part of the phenocryst assemblage of the high-temperature end-member magma. The modal amount of pyroxene with high Mg-number (Mg-number >78) is <0·1 vol. %. Other phenocrysts with low Mg-number (i.e. opx, hornblende, biotite, magnetite and ilmenite) are assumed to belong to the low-temperature magma. Most plagioclase cores show complex oscillatory zoning, ranging from An_{35} to An_{75} (Nakada & Motomura, 1999) with low MgO (<0·02 wt %) and FeO* (0·2–0·3 wt %) contents. These phenocrysts contain inclusions of other minerals, suggesting coprecipitation of most of the minerals; that is, plagioclase contains hornblende, biotite, magnetite, ilmenite and apatite inclusions. The plagioclase also contains glass inclusions, usually with bubbles.

Pyroxene thermometry

The compositions of minerals were analysed by electron microprobe at Hannover and Kobe Universities (for analytical conditions, see Table 1). The analyses of opx–cpx pairs observed as phenocrysts in the bulk rock have been used to calculate temperatures prevailing in the magmas (using QUILF, Lindsley & Frost 1992). We used a sample collected from a mudflow on 13 August 1992 (by H. Sato), probably originating from a pyroclastic flow from lava lobe number 7 (sample 92081301). Some opx phenocrysts show complex zoning (normal and inverse zoning; 'normal' zoning involves increasing Fe content from the core to the rim of the mineral). Only minerals with slight normal zoning or no zoning were selected for geothermometry. Eight pairs clearly consisted of adjacent and intergrown phenocrysts of opx and cpx (grey dots in Fig. 2). The temperatures calculated from the analysis of the rims of the adjacent opx and cpx are in the range 1055 ± 75°C (Table 1a). Six pairs yielded temperatures between 1030 and 1130°C. Most isolated phenocrysts, either opx or cpx, have compositions that plot in the same field as the opx–cpx pairs (black dots in Fig. 2), especially the opx. In contrast, most of the pyroxenes in the groundmass have higher Fe contents and a temperature of 930°C is calculated from the average value of all opx (58 analyses) and all cpx (11 analyses) analysed in the groundmass (open circles in Fig. 2). We interpret the temperature of 1055°C ± 75°C as representative of that of the high-temperature andesitic magma, prior to the mixing event with the low-temperature magma. This interpretation also predicts that the andesitic magma was not completely aphyric, in contrast to previous assumptions. The temperature of 930°C obtained from the groundmass pyroxenes is in agreement with the estimated post-mixing temperature by oxide thermometry of 900 ± 30°C (Venezky & Rutherford, 1999).

The compositions of opx–cpx pairs from a dark andesitic enclave collected from the top of Unzen volcano (spine extruded in 1994) have also been determined. It is emphasized that the dark enclaves in Unzen rocks show a wide range in bulk composition (basaltic to andesitic; Nakada & Motomura 1999) and that they do not necessarily represent the composition of the high-temperature magma involved in the 1991–1995 eruption. However, in the case of the investigated enclave, the analytical results given in Table 1b indicate an average temperature of 1050°C ± 26°C, which is close to that determined from phenocrysts in the bulk dacitic rock.

Analysis of untreated glass inclusions (major elements and water)

The major element compositions of glass inclusions in different phenocrysts collected from dome samples and from two volcanic bombs have been analysed by electron microprobe. The glass inclusions are generally vesiculated and include a gas bubble (see also Yamaguchi, 1997). Inclusions from the dome samples are sometimes also partially crystallized with the formation of alkali feldspar at the rim or with crystallization of tiny Fe-rich phases within the inclusion (too small to be analysed by microprobe). The average major element composition of glass inclusions is given in Table 2. It is emphasized that the results are rather qualitative and do not strictly represent the melt composition at the time when the inclusions were formed, first because the melt inclusions suffered at least one heating event through magma mixing (and therefore partial dissolution of the host mineral should occur), second because of possible partial crystallization (as a result of slow cooling, especially in the external lava lobes), and third because of possible leaks and loss of volatiles. When compared with glass inclusions in plagioclase, the high SiO_2 contents of inclusions in quartz and the high CaO and FeO contents of inclusions in amphibole confirm the possible dissolution of the host mineral after entrapment. The compositions of inclusions in two plagioclases from volcanic bombs from 1991 are probably the most representative of quenched melts unaffected by slow cooling processes (rapid ascent is expected in the bombs). The comparison between the glasses analysed in plagioclases of the bombs and in plagioclases of the dome shows that the CaO and Al_2O_3 contents are higher, and Na_2O and K_2O lower, in the glasses of the bombs, which can be explained by partial crystallization of An-rich plagioclase at the interface between the melt inclusion and the host mineral in samples that cooled slowly. Another possible explanation is that the compositions of melts trapped in the analysed plagioclases from the bombs and from the dome were different. In any case, all inclusions in plagioclase clearly have a rhyolitic composition [as already noted by

Table 1a: Compositions of clinopyroxene–orthopyroxene phenocryst pairs in the Unzen bulk dacite

No.:	2.3 cpx	2.4 opx	2.10 cpx	2.11 opx	2.12 cpx	2.13 opx	2.23 cpx	2.24 opx	3.3 opx	3.4 cpx	3.10 opx	3.11 cpx	4.43 cpx	4.44 opx	4.54 cpx	4.55 opx
SiO_2	52·26	54·84	51·11	53·29	50·53	53·16	52·16	54·31	52·66	49·70	52·78	50·89	52·16	55·28	54·12	52·41
TiO_2	0·28	0·15	0·41	0·18	0·36	0·19	0·29	0·14	0·23	0·80	0·26	0·40	0·37	0·16	0·19	0·30
Al_2O_3	1·94	1·06	2·95	1·89	2·71	1·80	1·63	1·49	2·70	4·64	2·87	2·22	2·63	1·34	2·47	2·53
FeO	5·93	11·96	6·12	11·64	6·08	12·00	7·09	12·73	13·20	8·21	15·33	11·33	6·26	12·12	12·25	5·97
MnO	0·19	0·25	0·15	0·37	0·17	0·25	0·34	0·29	0·36	0·17	0·26	0·39	0·14	0·32	0·34	0·19
MgO	16·50	29·13	15·89	28·70	16·26	29·60	16·87	28·79	25·78	15·11	25·19	16·90	16·63	29·28	28·44	16·60
CaO	20·86	1·36	21·00	1·36	20·65	1·32	19·86	1·22	2·71	19·66	1·93	15·15	21·45	1·48	1·61	21·24
Na_2O	0·23	0·04	0·30	0·01	0·28	0·03	0·23	0·09	0·07	0·31	0·02	0·22	0·30	0·01	0·05	0·29
K_2O	0·00	0·00	0·02	0·02	0·01	0·00	0·01	0·00	0·02	0·02	0·00	0·10	0·01	0·03	0·01	0·00
Total	98·20	98·79	97·94	97·45	97·04	98·35	98·47	99·06	97·71	98·62	98·64	97·60	99·93	100·02	99·48	99·53
*X*Mg	0·85	0·82	0·86	0·83	0·88	0·86	0·84	0·82	0·78	0·81	0·75	0·75	0·88	0·82	0·82	0·87
En	46·83	78·71	45·53	78·80	46·49	79·02	47·37	77·61	72·78	43·99	71·26	48·77	46·16	78·41	77·44	76·49
Fs	9·76	18·51	10·08	18·50	10·04	18·35	11·71	19·71	21·48	13·69	24·76	18·98	9·97	18·70	19·24	9·68
Wo	42·57	2·65	43·26	2·67	42·43	2·53	40·09	2·37	5·50	41·15	3·92	31·42	42·80	2·85	3·15	42·77
Jd/Ae	0·84	0·13	1·13	0·03	1·04	0·10	0·83	0·31	0·24	1·17	0·07	0·83	1·07	0·05	0·17	1·07
QUILF *T* (°C)	1032		1060		1072		1036		1128		1139		987		974	

Table 1b: Compositions of clinopyroxene–orthopyroxene phenocryst pairs in the Unzen dark enclave

No.:	22.1 cpx	22.5 opx	22.2 cpx	22.6 opx	22.3 cpx	22.7 opx	22.4 cpx	22.8 opx	22.17 cpx	22.18 opx	22.12 cpx	22.13 opx
SiO_2	50·65	53·56	49·31	53·16	51·65	53·33	50·15	54·37	51·80	54·78	51·86	54·92
TiO_2	0·69	0·24	0·91	0·32	0·51	0·15	0·67	0·15	0·40	0·21	0·39	0·15
Al_2O_3	3·84	2·51	4·71	2·51	2·45	0·93	3·93	1·27	2·42	1·53	2·34	1·18
FeO	6·97	12·18	6·92	13·33	7·83	15·86	6·73	12·71	5·80	11·75	6·43	11·81
MnO	0·17	0·36	0·14	0·21	0·28	0·41	0·18	0·41	0·17	0·38	0·23	0·23
MgO	15·70	28·95	14·77	27·56	17·02	26·46	15·79	29·03	16·48	29·15	17·12	29·31
CaO	21·20	1·35	21·81	1·45	18·76	1·27	20·96	1·32	21·71	1·55	20·58	1·52
Na_2O	0·27	0·04	0·30	0·04	0·27	0·02	0·24	0·03	0·23	−0·004	0·23	0·05
K_2O	0·01	0	0	0·01	0·02	0·01	0	0·02	0·02	0	0	0·01
Total	99·51	99·19	98·86	98·59	98·80	98·45	98·64	99·33	99·02	99·36	99·16	99·17
*X*Mg	0·69	0·70	0·68	0·67	0·69	0·63	0·70	0·70	0·74	0·71	0·73	0·71
En	52·89	80·87	52·98	77·33	53·28	74·35	53·94	80·04	52·40	79·47	54·32	79·89
Fs	8·74	16·30	8·06	19·64	11·10	23·03	8·26	17·27	7·51	17·43	7·51	17·09
Wo	38·37	2·83	38·96	3·03	35·62	2·62	37·80	2·69	38·17	3·10	38·17	3·02
QUILF *T* (°C)	1073		1044		1021		1053		1045		1068	

All analyses performed at the University of Hannover; analytical conditions: 15 kV, 15 nA, 10 s counting time on peak position, 5 s counting time on background, focused beam size. Standards: wollastonite for Si and Ca; $MnTiO_3$ for Ti and Mn; corundum for Al; haematite for Fe; periclase for Mg; albite for Na; orthoclase for K.

Nakamura (1995)] with relatively low FeO and MgO contents and high SiO_2 contents (>75 wt %).

The determination of water concentration in the glasses of the inclusions was made from the electron microprobe analyses using the 'by-difference' method (e.g. Devine *et al.*, 1995). The analytical conditions are given in Table 2. The analyses were made with a defocused beam of 10–15 μm diameter. For each microprobe

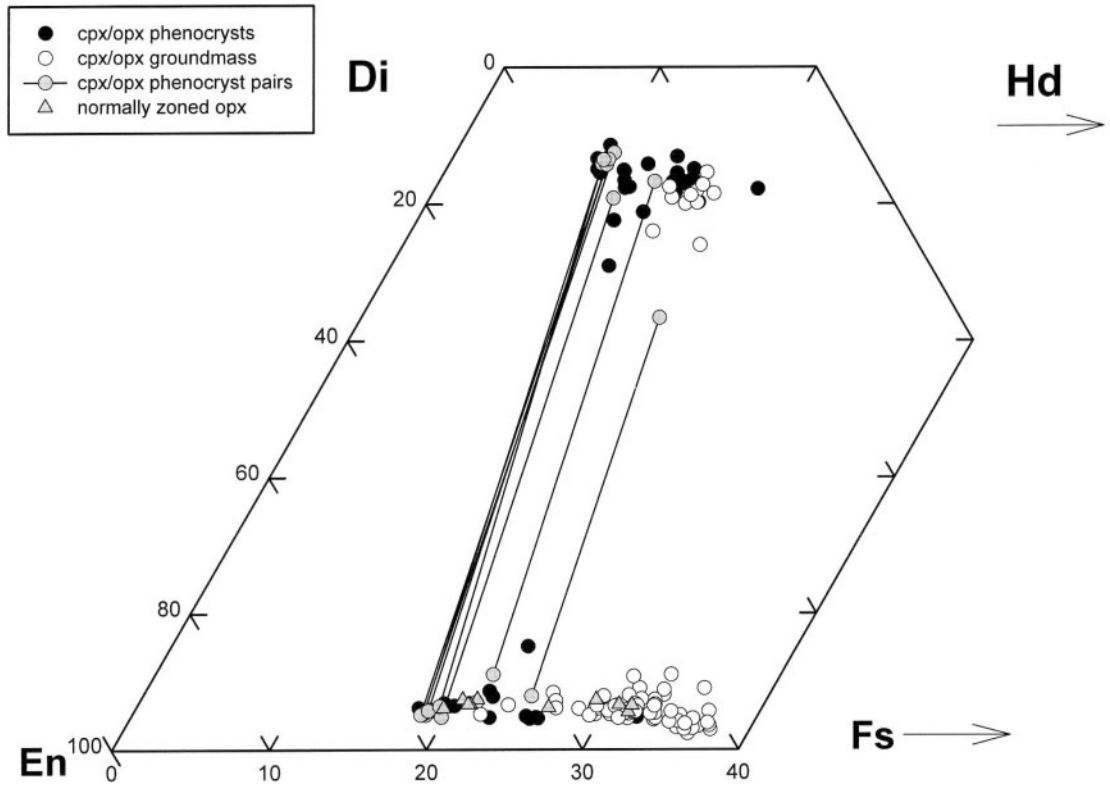

Fig. 2. Normative compositions of orthopyroxene and clinopyroxene in Unzen dacite in the system Di–Hd–En–Fs [thin sections from one sample (92081301) collected in a mudflow on 13 August 1992]. Grey dots and tie-lines, opx–cpx pairs; •, isolated phenocrysts; ○, minerals from the groundmass; grey triangles, opx with normal zoning. The analysed sample has also been used as the starting material for the experimental study (see composition in Table 2).

analytical session, we determined the difference from 100% for synthetic rhyolitic glasses with known water contents (containing up to 6·6 ± 0·15 wt % H_2O; the water contents of the standard glasses were detemined by Karl Fischer titration [see Holtz *et al.* (1995) for this technique and for the analytical precision] and a calibration curve was made to recalculate the water contents in the glasses. Table 2 presents analytical results obtained for glasses in three plagioclases in three samples (up to 12 inclusions in one plagioclase). The analytical total for each glass analysis (shown as 'sum' in Table 2) was very high, and the average water contents in the glasses, determined by the difference method, were found to be 1·9 and 2·8 wt % H_2O for the inclusions in two plagioclases from bombs (see microprobe analyses made at Hannover in Table 2). This low water content may be due to diffusion of water into the gas bubble of the inclusion during magma ascent or to leakage of the inclusions during ascent.

Analysis of annealed glass inclusions

Assuming that part of the water trapped in the glass inclusions may be concentrated in the gas bubbles, some grains of plagioclase were separated from the dacite and annealed under pressure at 850°C. Total water content present in glass inclusions was subsequently analysed. The selected minerals were placed together with rounded quartz crystals in a sealed gold capsule after drying at 70°C for more than 12 h (the rounded quartz was placed in the capsule to avoid damage to the capsule wall by sharp pieces of plagioclase). The gold capsule was heated to 850°C and 200 MPa for 8 h in a cold-seal pressure vessel pressurized with argon [for detailed description of the vessel, see Holtz *et al.* (1995)]. With this procedure, water present in the vesicle should dissolve back into the melt and remain in the glass during quenching. Because the samples are pressurized with argon, no water can penetrate into the melt inclusions if they are not sealed (cracks through the host mineral), but it is expected that such inclusions will lose their volatiles. After this high-pressure–high-temperature treatment, the plagioclases were prepared for microprobe analysis. The microprobe analyses of the annealed inclusions were made with a defocused beam (Table 2) and, when possible, several analyses were performed on each inclusion, avoiding any overlap between the analysed spots. When compared with the composition of the starting glasses, the CaO and

Table 2: Compositions of starting materials and glass inclusions

	Whole-rock analyses		Microprobe analyses of glass inclusions							
	Bulk[1]	Groundmass[2]	quartz[3]	amph[3]	plag.dome[3]	in one plag.dome[4]	in one plag.bomb[5]	in one plag.bomb[5]	inclusion G1 after heating[6]	inclusion G2 after heating[6]
n:	1	1	15	17	9	14	55	42	12	11
SiO_2	64·58 (65·10)	68·24	80·58	74·59	75·98	76·82	76·30	76·36	76·12	76·25
TiO_2	0·70 (0·65)	0·53	0·10	0·33	0·15	0·18	0·19	0·18	0·14	0·17
Al_2O_3	15·84 (15·59)	14·95	10·40	13·95	13·00	11·91	13·57	13·38	15·28	15·36
FeO*	5·04 (4·81)	4·05	0·79	1·64	0·81	1·19	0·84	0·91	0·80	0·73
MnO	0·09 (0·10)	0·09	0·04	0·05	0·05	0·07	0·08	0·04	0·05	0·04
MgO	2·65 (2·48)	1·91	0·13	0·21	0·14	0·13	0·12	0·15	0·15	0·11
CaO	4·86 (5·11)	3·86	0·92	1·51	1·20	0·94	1·21	1·38	3·16	3·08
Na_2O	3·61 (3·45)	3·48	3·07	2·81	4·36	3·85	3·73	3·73	3·08	3·12
K_2O	2·50 (2·49)	2·85	3·98	4·90	4·29	4·82	3·96	3·87	1·22	1·14
P_2O_5	0·14 (0·22)	0·14	n.a.	n.a.	n.a.	n.a.	n.a.	n.a.	n.a.	n.a.
Total	100·00	100·00	100·00	100·00	100·00	100·00	100·00	100·00	100·00	100·00
Σ microprobe		95·92	96·64	95·64	98·1[7]	97·2[7]	98·2[7]	91·8[7]	91·5[7]	

n, number of analyses; n.a., not analysed.
*Total Fe given as FeO.
[1]Starting material for the experiments; sample 92081301A; analysis by inductively coupled plasma mass spectrometry; data given in parentheses are average values obtained by microprobe analysis of the dry glass (made from the natural sample).
[2]Groundmass composition of the Unzen dacite after Sato *et al*. (1999).
[3]Average composition of glass inclusions in several phenocrysts (microprobe analysis, Kobe; analytical conditions are given in the text).
[4]Average composition of glass inclusions in one plagioclase phenocryst of a sample of 1992 (microprobe analysis: Hannover; analytical conditions: 15 kV, 6 nA, 5 s counting time, Na analysed first, beam size defocused to a diameter between 10 and 15 μm).
[5]Average composition of glass inclusions in one plagioclase phenocryst of a bomb from 1991 (microprobe analysis: Hannover).
[6]Composition of one glass inclusion in plagioclase after heating at 850°C and 200 MPa (microprobe analysis: Hannover). The plagioclase was collected from sample 92081301A.
[7]Sum of microprobe analyses made at Hannover were calibrated against standard samples containing up to 6·6 wt % H_2O.

Al_2O_3 content of the inclusions after heating was significantly higher and the K_2O content was lower. This is interpreted to be due to a reaction between the host plagioclase and the melt during the experiment. Many inclusion glasses showed totals close to 100%. For some of these inclusions, cracks propagating from the inclusion into the host mineral could be observed, suggesting that all or a part of the fluid may have escaped during the annealing experiment. On the other hand, some inclusions showed low microprobe analysis totals. Two of these inclusions, with a size of *c.* 150 μm in diameter, were selected for detailed microprobe analysis. The water content estimated 'by difference' by microprobe (Table 2) was found to be very high, with an average value of 8·2 wt % H_2O (inclusion G1; 12 analyses in the range 7·0–9·0 wt % H_2O) and 8·5 wt % H_2O (inclusion G2, 11 analyses in the range 7·8–9·6 wt % H_2O).

One of these glass inclusions (G1) was subsequently analysed using Raman microspectroscopy following the method described by Thomas (2000). This technique allows for the collection of spectra in very small volumes of sample. A confocal Raman spectrometer equipped with a microscope and a 50× long distance objective was used. The samples were excited with the 532 nm line of a Nd–Y–Ag-laser operating at a power of 100 mW at the source. The laser-beam diameter was focused to ~2 μm below the surface of the sample. Acquisition time was 50–100 s. The integrated intensity of the Raman band at ~3600 cm^{-1}, resulting from the stretching vibrations of both molecular water and hydroxyl groups, has been determined in the glass inclusion and in six haplogranitic standard glasses with water contents ranging from 10·7 to 1·3 ± 0·15 wt % H_2O. Using these standard samples, a linear calibration curve between the integrated band intensity at 3600 cm^{-1} and the total water content of the standard glasses was established [see also Thomas (2000)]. The standard samples were continuously analysed during the analytical session to correct for small

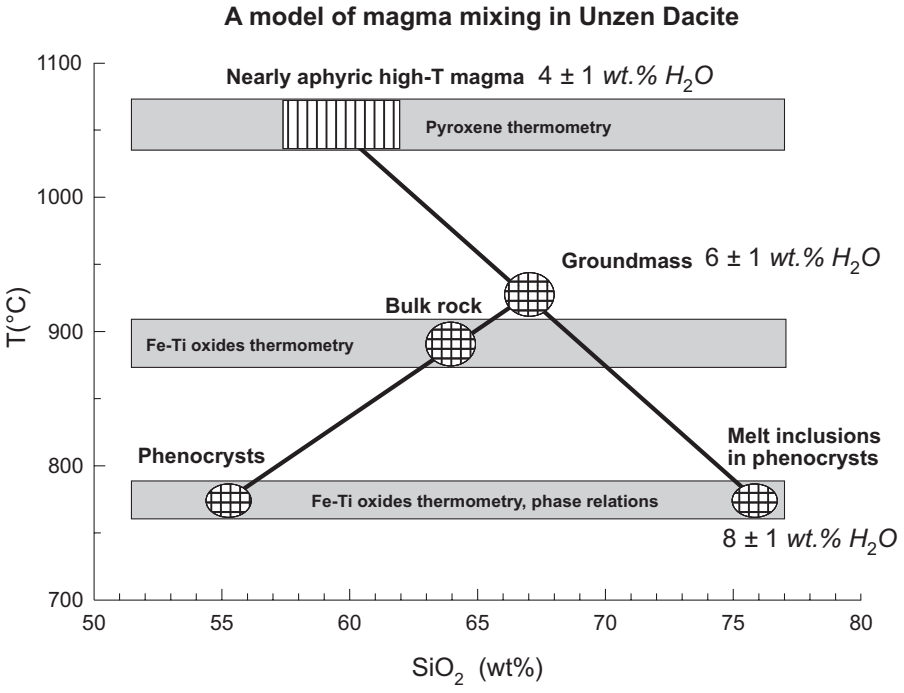

Fig. 3. A model of magma mixing for the 1991–1995 dacite of Unzen volcano. The SiO_2 contents of the groundmass, of glass inclusions and of a typical bulk-rock composition are given in Table 2. Following this model, the bulk dacite is composed of *c.* 30 wt % phenocrysts, 35 wt % rhyolitic melt ($T \sim 775°C$) and 35 wt % andesitic magma (almost aphyric, $T \sim 1050°C$). The water content of the melt in the low-temperature magma and in the melt after mixing (groundmass) is estimated from the analysis of glass inclusions and from phase relationships at 300 MPa, respectively. The water content in the high-temperature magma is estimated assuming that the groundmass results from the mixing of 50% rhyolitic melt and 50% high-temperature melt.

shifts from the calibration curve with time (preliminary investigations to test the reliability of this method showed that a continuous recalibration was necessary). Twelve spectra were collected at different positions on the glass inclusion and the calculated water contents varied in the range 6·9–10·5 wt % H_2O, with an average water content of 8·5 wt % H_2O. These results from Raman spectrometry on glass inclusion G1 are in good agreement with microprobe analyses for the same inclusion (8·2 wt % H_2O).

The glass analyses show the presence of very high water contents in the inclusions. Assuming that the analysed inclusions were composed only of a pure melt phase (no free fluid) when they were trapped in the host minerals, a minimum pressure at which the inclusions were formed can be determined. The incorporation of 8 wt % H_2O in melts can occur only at pressures above 300 MPa in rhyolitic melts (the water solubility in rhyolitic melts is between 7 and 8 wt % at 300 MPa; e.g. Holtz *et al.*, 1995). This pressure is a minimum value because water solubility is even lower if an additional volatile such as CO_2 is dissolved in the melt (e.g. Blank *et al.*, 1993; Tamic *et al.*, 2001). Other volatiles such as Cl, which are known to be dissolved in significant amounts in melts from Unzen (up to 850 ppm; Yamaguchi 1997) are not expected to change the water solubility significantly (e.g. Webster *et al.*, 1999). It is emphasized that the water contents of these two inclusions are not necessarily those of the rhyolitic melt involved in the mixing process prior to the 1991–1995 eruption (the inclusions could be older). However, our results show that melts with extremely high water contents may have prevailed at some stages of the history of Unzen volcano. Considering that the maximum depth for the storage of the rhyolitic end-member is 11 km (Nishi *et al.*, 1999), it can be concluded that these melts were probably saturated with respect to a water-rich fluid prior to the mixing event.

A magma mixing model for the 1991–1995 dacite of Unzen volcano

Figure 3 represents a general model for magma mixing in the 1991–1995 dacite. This model can be considered as a simplified working hypothesis (volatiles other than water have not been considered), synthesizing our present knowledge on the last Unzen eruption. It is modified after that of Nakamura (1995, 1996) with new constraints on the temperature of the high-temperature magma, on the temperature of the phenocryst-rich low-temperature end-member magma [estimated by Venezky & Rutherford (1999) to be around 790°C], and on the temperature of the mixed dacite (estimated from the

compositions of the groundmass iron–titanium oxides to be 900 ± 30°C; Venezky & Rutherford, 1999). The chemical composition of the phenocryst assemblage is estimated from the composition of individual phenocryst minerals (mainly plagioclase and amphibole) and their modal proportions (Nakamura, 1996). The melt composition of the low-temperature magma is estimated from the composition of glass inclusions in the plagioclase phenocrysts (data in Table 2), leading to an SiO_2 content of 76–77 wt % (anhydrous basis). In Fig. 3, the SiO_2 content of the high-temperature magma was obtained graphically by extending the straight line connecting the SiO_2 content of the groundmass composition (Table 2) and of the glass inclusions up to 1050°C. Assuming that 1050 ± 25°C is the temperature of the mafic end-member, that the mafic magma is mainly composed of melt (almost aphyric) and that the groundmass composition results from the mixing of the low- and high-temperature melts, the SiO_2 content of the high-temperature magma can be constrained at 60 ± 2 wt % SiO_2. Such nearly aphyric pyroxene-bearing andesite–dacites (SiO_2 60–67 wt %) occur in the Pliocene–Pleistocene formations in the surrounding areas in NW Kyushu.

In this model, the groundmass of the dacite is considered to result from the mixture of the bulk rock of the high-temperature magma and the melt fraction of the low-temperature magma (specific heat and heat of mixing have been neglected). The high-temperature magma is almost aphyric, except for a few pyroxenes with high Mg-number (the amount of these pyroxenes must be low, considering that their volume in the mixed magma is around 0·1 vol. %). Assuming that the SiO_2 contents of the high- and low-temperature melts are ~60 and 75 wt %, respectively, a simple mass balance calculation indicates that the proportions of the high-temperature andesitic magma and low-temperature silicic melt necessary to form the groundmass composition are nearly equal, which is consistent with the conditions required for magma mingling proposed by Sparks & Marshall (1986) and with estimates based on sulphur concentrations in glass inclusions (Satoh *et al.*, 2003). Thus, assuming a total phenocryst content of 30 wt %, the proportions of both rhyolitic and andesitic melts would be *c.* 35 wt % each. It is emphasized that the amount of phenocrysts was not constant during the 1991–1995 eruption process (varying from *c.* 23 to 28 vol. %; Nakada & Motomura, 1999). Thus, the proportions given above can only be estimates.

EXPERIMENTS

Starting material

Crystallization experiments were performed with a glass corresponding to the Unzen dacite composition (Table 2) to constrain the conditions prevailing in the magma chamber prior to eruption. The water content of the melt was of particular interest and the experiments were, therefore, carried out at various water activities. Most of the experiments were conducted at 300 MPa, a pressure corresponding to that of the depth at which magma mixing is supposed to have occurred.

Table 2 shows the major element composition of the starting material, which is representative of the bulk Unzen dacite. The starting material was taken from a hot block of *c.* 2 m diameter recovered from the 13 August 1992 mudflow deposit in the Mizunashi river. The temperature obtained by IR camera recorded *c.* 500°C at a distance of 10 cm from the surface of the block, suggesting that the block was recently derived from the active lava dome via a pyroclastic flow and subsequently incorporated into a mud flow. The powder of the bulk rock was fused at 1600°C in a Pt crucible for 5 h under atmospheric conditions (no significant loss of alkalis occurred with this procedure; see glass analysis in Table 2). The cooled glass was powdered (grain size <60 μm) and inserted in Au or AgPd capsules with distilled water (water-saturated conditions) or with a mixture of H_2O and silver oxalate ($Ag_2C_2O_4$). The use of silver oxalate results in the reduction of the water activity at constant pressure and temperature. The initial mole fraction of H_2O in the added fluids is listed in Table 3. The total volatile content (CO_2 and H_2O) was kept at 10 wt % of the total charge.

Experimental method

The experiments were conducted in externally heated cold seal pressure vessels for 7–10 days in the range 100–300 MPa and 750–875°C (Table 3). The vessels (Tuttle-type) are made of a nickel alloy and water was used as the pressurizing medium. Using the solid buffer technique, oxygen fugacity was kept at the Ni–NiO buffer during runs. Although the starting glass was prepared under oxidizing conditions, the time necessary to attain redox equilibrium conditions at the Ni–NiO buffer is relatively short using Au capsules of 2 mm thickness [21 h at 750°C; 9 h at 800°C; using the equations of Harvie *et al.* (1980)]. Thus, an experimental duration of 7–10 days is long enough to ensure equilibrium redox conditions. Chemical zoning in the crystalline phases was not observed (when the crystal size was large enough), suggesting that there was no significant growth of crystals before the equilibrium oxidation state was established (or that crystals reacted with changing oxygen fugacity in the beginning of the experiments). After the runs, the vessels were cooled by an air flux, allowing a cooling rate of *c.* 300°C within 1 minute. The temperature was regulated within 10°C, and pressure was kept within 5% of the nominal values [for further details, see Holtz *et al.*

Table 3: Experimental conditions and results of the determination of phase equilibria

Run	Temperature (°C)	Pressure (MPa)	$X(H_2O)$[1]	H_2O in melt[2] (wt %)	Phases[3]
1	825	300	1·00	7·6	pl (8), amph (18), ilm (tr), gl (73)
1–2	825	300	0·78	6·8	pl (31), amph (11), ilm (1), opx (5), gl (52)
2	825	300	0·79	6·8	pl (31), amph (9), ilm (1), gl (6), gl (53)
3	800	300	1·00	7·6	pl (15), amph (17), ilm (tr), ap(tr), gl (68)
4	800	300	0·80	6·7	pl (34), amph (12), ilm (1), opx(3), gl (50)
5	825	300	0·61	5·3	pl (38), ilm (tr), opx (9), qz (2), gl (50)
7	850	300	1·00	7·5	pl (4), amph (16), ilm (tr), gl (80)
8	850	300	0·78	6·9	pl (29), amph (7), ilm (1), opx (7), gl (56)
9	850	300	0·59	5·4	pl (40), ilm (1), opx (12), gl (47)
10	850	300	0·40	4·1	pl, ilm, cpx, opx, qz, gl (*)
11	775	300	1·00	7·6	pl (17), amph (16), ilm (tr), bt (2), gl (63)
12	775	300	0·79	6·6	pl (24), amph (22), ilm (1), gl (52)
13	850	200	1·00	6·2	pl, amph, ilm, gl (*)
14	850	200	0·80	4·5	pl (26), opx (12), ilm (tr), gl (61)
15	850	200	0·59	3·2	pl (35), opx (13), ilm (1), gl (51)
16	850	200	0·41	1·8	pl, amph, qz, gl (*)
17	875	300	1·00	7·5	amph (12), mt (2), gl (89)
18	875	300	0·79	6·5	pl, amph, opx, mt, gl (*)
19	875	300	0·60	4·7	pl (22), opx (8), mt (3), gl (67)
20	875	300	0·40	3·6	pl, amph, gl (*)
25	850	100	1·00	4·2	pl (25), opx (12) ilm (tr), gl (62)
26	850	100	0·78	3·7	pl, amph, opx, mt, gl (*)
29	825	200	1·00	6·2	pl, amph, mt, gl (*)
30	825	200	0·79	4·5	pl, amph, opx, mt, gl (*)
50	800	200	1·00	6·2	pl (20), amph (17), mt (1), gl (62)
51	800	200	0·80	4·5	pl (34), amph (13), opx (4), mt (tr), gl (48)

pl, plagioclase; amph, amphibole; cpx, clinopyroxene; opx, orthopyroxene; bt, biotite; qz, quartz; mt, magnetite, ilm, ilmenite; ap, apatite; gl glass; tr, traces.
*Phase proportions were not calculated because only compositions of some phases were analysed.
[1]Mole fraction of water in the fluid (composed of H_2O and CO_2) in the starting material.
[2]Water content of melts (see text).
[3]Modal composition in wt % calculated after the least-squares method (Sugawara, 1998).

(1995)]. After the experiments, the capsules were checked by weighing, and presence of a gas phase was ascertained by checking the leak of fluid when opening the capsules. The run products were analysed by electron microprobe [University of Kobe; for analytical conditions, see below and Sato *et al.* (2005)].

Phase relations

Phase assemblages in the experimental runs are summarized in Table 3 and Fig. 4. Particular attention was given to the presence of plagioclase, amphibole, ortho- and clinopyroxene, quartz and biotite. Clinopyroxene was not observed at the investigated conditions ($T <$ 875°C). Ilmenite, magnetite and apatite were observed in some runs (Table 3), but we did not check systematically for their occurrence. Thus, these minerals may also be present in runs in which they have not been recognized. Figure 4 shows the phase relations (oxides and apatite excluded) in terms of temperature versus the water content of the melt at 300 MPa. The water contents were calculated by different methods. For experiments with $X(H_2O) = 1·0$, the water content was calculated from water solubility models for rhyolitic melts (Holtz *et al.*, 2001). For $X(H_2O) < 1·0$, the water contents were estimated from the data of Dall'Agnol *et al.* (1999) and Klimm *et al.* (2003), who performed crystallization experiments on A-type granites (70–72 wt % SiO_2) at 300 and 200 MPa, using the same experimental method (and the same amount of added fluid). In these studies the water content of the glasses was estimated by microprobe analysis following the difference method described by Devine *et al.* (1995) and a calibration of the method was made

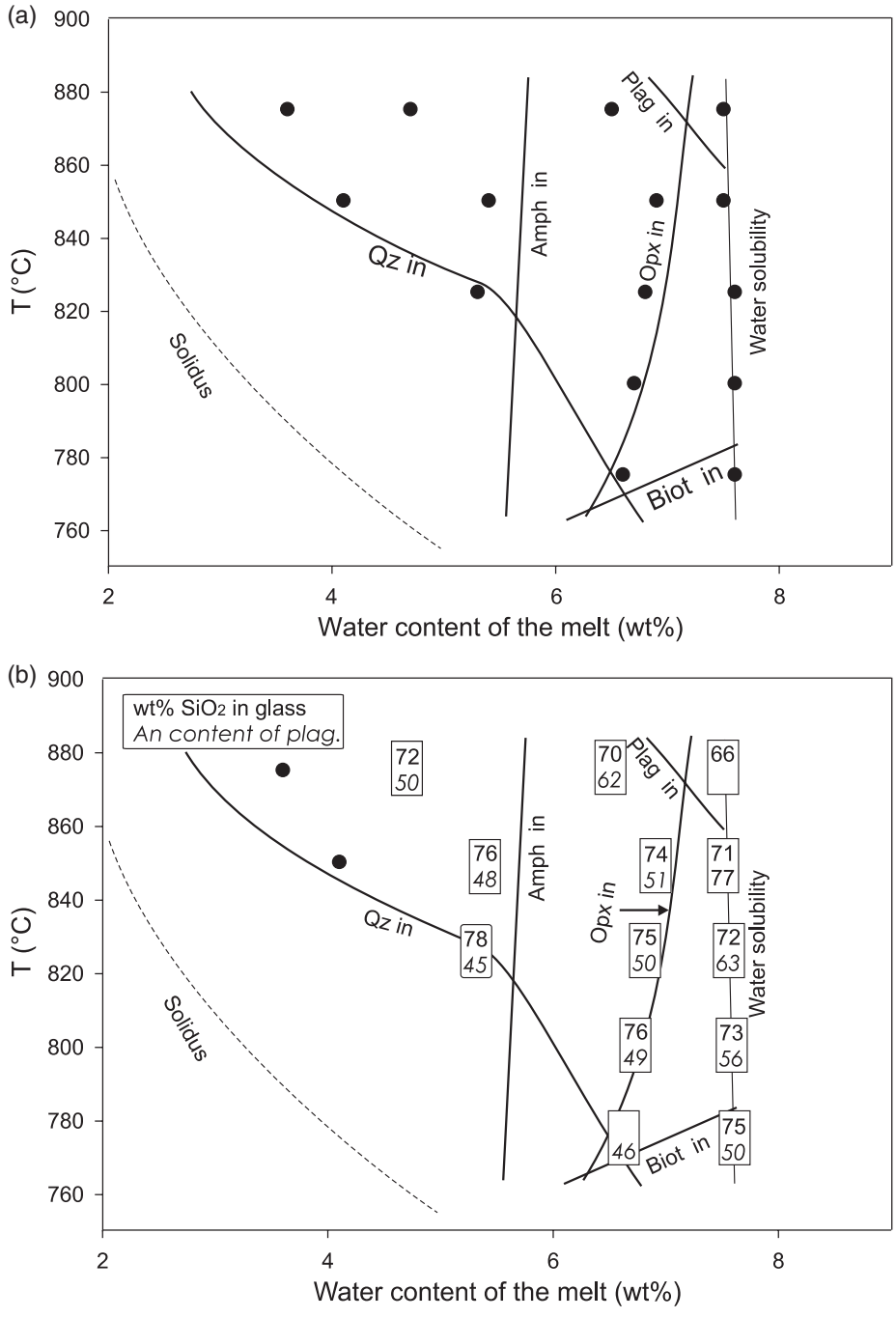

Fig. 4. Experimental phase relationships of Unzen dacite at 300 MPa, Ni–NiO buffered conditions as a function of temperature and water content of the melt. The phases ilmenite and magnetite are not represented and have not been identified systematically in the run products. (a) •, experimental conditions. (For the determination of the water content of the melt, the solidus and the water solubility curve, see text.) (b) The upper number in the rectangle represents the SiO_2 content of the glasses (in wt %, recalculated to a sum of 100%) and the lower number is the An content of plagioclase analysed in the experimental products. Data are given in Tables 3 and 4.

using standard glasses with known water contents. Because the starting material contains less SiO_2 than granitic compositions, the crystal amounts in our experimental products are higher than those obtained by Dall'Agnol *et al.* (1999) and Klimm *et al.* (2003). Thus, the amount of free fluid phase is higher in our experiments and the $X(H_2O)$ in the fluid after the experiments is also higher (water dissolves preferentially in the silicate

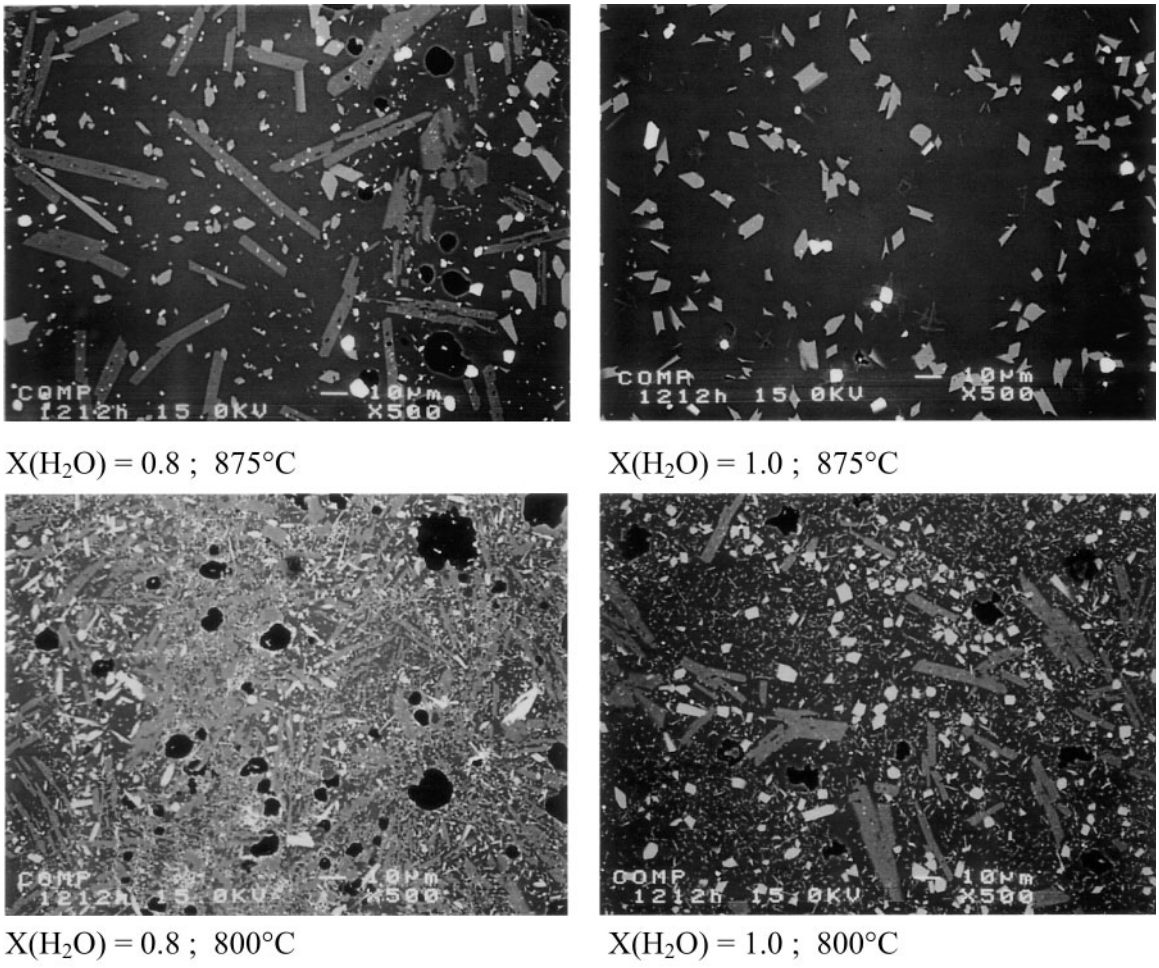

Fig. 5. Back-scattered electron images of some experimental products as a function of $X(H_2O)$ and temperature. The brightest minerals represent oxides (magnetite or ilmenite), the next bright minerals are either hornblende or pyroxene, and dark rectangular minerals are plagioclase. The glass matrix is dark. The widths of the photographs are 200 μm.

melt when compared with CO_2). This means that the estimated water contents given in Table 3 are minimum values for experiments with $X(H_2O) < 1{\cdot}0$.

Representative back-scattered electron (BSE) images of the experimental charges are shown in Fig. 5. The right-hand side photographs in Fig. 5 are the BSE images for $X(H_2O) = 1{\cdot}0$, and the left-hand side photographs are for $X(H_2O) = 0{\cdot}8$. Clearly, the crystallinity of the products increases as temperature rises and $X(H_2O)$ decreases. Some of the BSE photographs show heterogeneous crystal distribution in the charge at lower temperatures (e.g. at 800°C), which may be due to undercooling effects. Crystals are generally euhedral in shape, and show no detectable compositional zoning.

Figure 4 shows that, at 300 MPa, the crystallization temperature of plagioclase ($An_{77–45}$) at water-saturated conditions [$X(H_2O) = 1{\cdot}0$] is slightly below 875°C. Amphibole is stable only at $X(H_2O) \geq 0{\cdot}8$ or for melt water contents higher than 5·0–6·5 wt % H_2O, whereas opx occurs only at water-undersaturated conditions with melt water contents below 7·5 wt % H_2O. Biotite is present only in the run at 775°C and $X(H_2O) = 1{\cdot}0$. No attempts were made to determine the solidus temperature at 300 MPa. The solidus line was drawn in Fig. 4 by combining the experimental data of Ebadi & Johannes (1991) and Holtz *et al.* (2001) for a haplogranitic system.

Biotite has not been observed at 100 and 200 MPa (Table 3). The experiments at these pressures were conducted at 800°C and above, suggesting that biotite in the Unzen dacite composition is stable at temperatures below 800°C. The effect of water activity on the biotite stability field is difficult to predict. Depending on bulk composition and pressure, the crystallization of biotite may increase or decrease with decreasing water activity (e.g. Dall'Agnol *et al.*, 1999; Klimm *et al.*, 2003). However, in any case, biotite is not expected to be stable at

temperatures much higher than 800°C in a dacitic composition such as that occurring at Unzen. Quartz stability is limited to low $X(H_2O)$ and low temperatures. This mineral has been observed only at 300 MPa, 825°C and $X(H_2O) = 0{\cdot}6$, and at 200 MPa, 850°C and $X(H_2O) = 0{\cdot}4$. In both cases, the conditions are close to the solidus, suggesting that quartz is the last phase to occur in the crystallization sequence.

Phase compositions

Experimental run products and some natural dacite samples were analysed by JEOL Superprobe JXA-8900 in the Venture Business Laboratory of Kobe University. The analytical conditions were 15 kV accelerating voltage and 12 nA beam current. Most of the elements were analysed for 20 s at the X-ray peak, and with a 10 s counting time on both sides of the peak for background. ZAF corrections were made on the background corrected counts. For analyses of hydrous silicic glass, sodium analyses were limited to 4 s with a broad beam (usually 10 μm in diameter). The analytical results are shown in Table 4. Figure 4b shows the silica content of the glasses (recalculated on an anhydrous basis) and the An content of plagioclases [$= 100 \times Ca/(Ca + Na)$]. The SiO_2 content of the glasses generally increased (up to 78 wt %) and the An content of plagioclase decreased as temperature fell and $X(H_2O)$ decreased. The most calcic plagioclase was An_{77} and was obtained at 850°C and $X(H_2O) = 1{\cdot}0$. The composition of plagioclase in the other experiments ranged between An_{43} and An_{63} (Table 4). The Mg-number of hornblende in the experimental run products was in the range 0·53–0·77 and increased with rise in temperature (at 300 MPa). The Mg-number of most orthopyroxenes was in the range 0·54–0·59.

DISCUSSION

Pressure constraints for the low-temperature magma chamber

A major question in the case of Unzen volcano is the location of the magma chamber in which mixing took place. Ishihara (1993) pointed out the possible presence of magma pockets at depths of 5 and 8 km from geodetic levelling data, which could be the location of the low-temperature end-member magma. However, the volume of the magma pockets at 5 and 8 km is estimated to be less than *c.* 10^7 m^3, which is much smaller than the total volume of erupted material of 2×10^8 m^3. More than half of the erupted magmas are derived from the low-temperature magma, and we believe that such an amount of magma may have resided in the main chamber at a depth of 11 km as pointed out by Nishi *et al.* (1999). Our results confirm that at least some of the plagioclase phenocrysts present in the dacite must have been formed at *c.* 300 MPa (or more) because of the high water content (8 ± 1 wt % H_2O) observed in the reheated glass inclusions. The Al_2O_3 content of amphibole is also an indicator of pressure and could be helpful to constrain the pressure after mixing by analysing the rim of amphibole phenocrysts. However, this is tenuous because all phases required for the geobarometer (especially quartz) may not have been at equilibrium. It should be noted that amphibole rims have an Al_2O_3 content ranging from 10 to 12 wt % and an Mg-number of 0·65–0·75 (Sato *et al.*, 2005), which is identical to that of the experimental products obtained at 300 MPa and temperatures of 850–875°C. The Al_2O_3 content of the core of amphibole phenocrysts is lower (most of the cores contain 6–9 wt % Al_2O_3; Sato *et al.*, 2005), but the cores of these phenocrysts may have crystallized from a more differentiated composition (and at lower temperatures), which is confirmed by the glass inclusions in these amphiboles (Table 2). Using the calibration established by Johnson & Rutherford (1989), Venezky & Rutherford (1999) determined a pressure of crystallization of 160 ± 20 MPa for the crystallization of the hornblende cores. However, for amphibole compositions similar to those of Unzen volcano, Dall'Agnol *et al.* (1999) demonstrated that the calibration of Schmidt (1992) leads to a pressure higher by ∼100 MPa than that estimated using the geobarometer of Johnson & Rutherford (1989). Thus, the comparison of experimental results and natural amphiboles does not rule out a crystallization pressure as high as ∼300 MPa for amphibole cores and for amphibole rims.

Phase relations of the low-temperature magma and its crystallization conditions

As described above, phenocryst phases in the low-temperature end-member magma consist of plagioclase, hornblende, biotite, magnetite, ilmenite, quartz, opx and apatite. Figure 4 shows that at 300 MPa, the three most abundant minerals, plagioclase, amphibole and opx, are stable together only at $X(H_2O) = 0{\cdot}8$, which means at slightly reduced water activities. From the stability fields of opx and amphibole shown in Fig. 4, the corresponding water content in the melt is *c.* 5–7 wt % at 875–825°C. Thus, assuming that mixing occurred at 300 MPa and that the post-mixing temperature was 870°C or higher, the water content of the hybrid melt can be constrained at a value of 6 ± 1 wt % H_2O.

The complete natural phenocryst assemblage (opx, plagioclase, hornblende + quartz and biotite) has not been reproduced at 300 MPa. However, the extrapolation of the phase relationships to lower temperatures (Fig. 4) shows that the five mineral phases mentioned above should be stable at temperatures just below 775°C (probably 775–750°C) and for water contents of the melt in the

Table 4: Composition of the phases in the experimental products

Run	Phase	*n*	SiO_2	TiO_2	Al_2O_3	FeO	MnO	MgO	CaO	Na_2O	K_2O	Total	Mg-no.	Ca-no.
1	gl	4	64·89	0·24	14·36	2·00	0·03	0·40	2·89	3·17	2·54	90·52	0·26	0·34
	hb	6	47·24	1·58	11·74	14·05	0·25	11·11	10·12	1·69	0·82	98·58	0·58	0·77
	pl	2	55·16	0·06	28·42	0·52	0·02	0·09	11·77	3·77	0·44	100·24	0·24	0·63
1–2	gl	4	70·86	0·22	12·37	1·49	0·03	0·27	1·79	3·05	3·75	93·83	0·24	0·24
	hb	4	50·11	1·71	9·42	15·25	0·23	11·65	9·84	1·42	0·81	100·45	0·58	0·79
	pl	4	58·51	0·09	26·20	0·87	0·02	0·23	9·16	5·12	0·67	100·86	0·32	0·50
2	gl	4	70·62	0·25	12·69	1·48	0·05	0·28	2·07	3·04	3·76	94·24	0·25	0·27
	hb	4	47·81	1·56	11·19	14·25	0·27	12·30	10·04	1·64	0·77	99·83	0·61	0·77
	opx	4	53·08	0·17	1·60	25·43	0·69	18·72	2·06	0·12	0·05	101·91	0·57	0·91
	pl	4	58·96	0·38	25·46	1·41	0·02	0·22	8·87	4·98	0·73	101·02	0·22	0·50
3	gl	5	67·21	0·21	13·82	1·71	0·06	0·33	2·44	3·26	2·79	91·82	0·26	0·29
	hb	15	45·41	1·37	10·97	16·77	0·32	11·60	10·14	1·61	0·57	98·75	0·55	0·78
	pl	4	56·20	0·16	27·46	1·02	0·01	0·39	10·71	4·67	0·37	101·00	0·40	0·56
4	gl	6	71·29	0·22	11·96	1·35	0·04	0·28	1·63	2·81	3·80	93·37	0·27	0·24
	hb	6	47·97	1·73	8·36	17·63	0·27	12·10	9·44	1·29	0·59	99·38	0·55	0·80
	opx	2	52·16	0·18	1·54	26·72	0·82	17·76	1·37	0·05	0·05	100·65	0·54	0·94
	pl	7	58·71	0·24	25·59	1·19	0·01	0·34	8·77	5·07	0·67	100·58	0·33	0·49
5	gl	3	66·42	1·07	12·57	3·16	0·04	1·70	2·34	2·33	3·10	92·74	0·49	0·36
	opx	2	53·00	0·20	1·00	24·70	0·61	18·26	3·41	0·04	0·06	101·27	0·57	0·98
	pl	4	59·48	0·27	24·79	1·01	0·01	0·22	8·05	5·52	0·94	100·27	0·28	0·45
7	gl	5	63·57	0·32	14·68	2·18	0·07	0·40	3·23	3·27	2·39	90·12	0·25	0·35
	hb	11	45·43	1·90	11·42	13·59	0·23	12·64	10·97	1·81	0·71	98·69	0·62	0·77
	pl	4	51·69	0·03	31·06	0·49	0·02	0·11	14·66	2·48	0·30	100·84	0·29	0·77
8	gl	5	69·79	0·28	12·86	1·70	0·04	0·35	2·09	3·28	3·54	93·93	0·27	0·26
	opx	8	53·29	0·26	1·63	23·67	0·62	19·39	2·66	0·04	0·04	101·60	0·59	0·97
	pl	6	58·44	0·13	25·65	1·23	0·02	0·42	9·32	5·04	0·59	100·84	0·38	0·51
9	gl	3	72·35	0·25	12·10	1·49	0·04	0·41	1·55	2·84	4·16	95·19	0·33	0·23
	pl	4	58·92	0·22	25·32	1·00	0·04	0·40	8·70	5·18	0·75	100·51	0·41	0·48
10	gl	5	64·12	0·14	18·48	2·60	0·33	1·91	5·39	4·03	1·84	98·85	0·57	0·42
11	gl	5	67·38	0·15	13·28	1·25	0·04	0·22	2·40	2·59	2·61	89·94	0·24	0·34
	hb	4	45·76	1·56	12·23	16·75	0·33	10·61	10·42	1·61	0·74	100·01	0·53	0·78
	bt	2	37·39	2·82	16·06	19·03	0·14	12·39	0·07	0·59	9·75	98·24	0·54	0·06
	pl	6	57·73	0·10	26·52	1·00	0·02	0·50	9·54	5·33	0·41	101·15	0·47	0·50
12	gl	5	68·01	0·18	12·76	1·29	0·03	0·23	2·05	2·75	3·01	90·31	0·24	0·29
	hb	3	53·68	0·98	10·77	13·81	0·28	9·65	8·20	1·37	0·71	99·45	0·55	0·77
	pl	6	59·30	0·05	26·05	0·70	0·01	0·12	8·62	5·67	0·50	101·02	0·23	0·46
13	gl	6	67·35	0·29	18·52	2·33	0·06	0·43	2·84	3·57	2·88	98·31	0·25	0·31
	hb	6	45·20	1·93	11·03	14·73	0·26	12·90	10·67	1·71	1·03	99·46	0·61	0·78
	pl	3	54·82	0·08	27·69	1·01	0·01	0·13	11·44	4·12	0·63	99·93	0·19	0·61
14	gl	3	71·41	0·31	16·53	1·73	0·02	0·32	1·98	3·31	3·80	99·49	0·25	0·25
	opx	7	52·70	0·26	1·37	25·02	0·55	19·81	1·78	0·03	0·06	102·68	0·58	0·97
	pl	2	58·92	0·08	25·36	1·27	0·03	0·21	8·91	5·06	1·13	100·97	0·23	0·49
15	gl	3	74·40	0·33	15·50	1·53	0·03	0·29	1·40	2·97	4·48	100·95	0·25	0·21
	opx	1	53·16	0·31	0·73	26·97	0·60	19·62	1·44	0·02	0·09	102·94	0·56	0·97
	pl	1	59·32	0·06	25·28	0·56	0·00	0·04	8·68	5·25	0·58	100·76	0·11	0·48
17	gl	3	63·62	0·36	19·45	1·91	0·07	0·88	4·13	3·34	2·49	96·33	0·45	0·41
	hb	5	45·27	1·45	10·42	8·84	0·17	16·51	11·90	1·72	1·17	97·46	0·77	0·79

Table 4: continued

Run	Phase	*n*	SiO_2	TiO_2	Al_2O_3	FeO	MnO	MgO	CaO	Na_2O	K_2O	Total	Mg-no.	Ca-no.
18	gl	4	68·56	0·34	17·91	1·77	0·05	0·72	2·81	3·48	2·96	98·67	0·42	0·31
	hb	5	46·67	1·58	10·41	9·92	0·25	16·08	10·99	1·74	1·09	98·75	0·74	0·78
	opx	1	53·15	0·30	3·88	12·53	0·64	27·32	2·66	0·26	0·14	100·86	0·80	0·85
	pl	3	54·62	0·08	27·80	1·40	0·03	0·40	11·53	4·12	0·61	100·58	0·34	0·61
19	gl	3	72·62	0·28	16·54	1·46	0·05	0·58	2·12	3·36	3·80	100·89	0·14	0·26
	opx	1	54·72	0·16	2·20	14·60	0·83	28·42	1·43	0·00	0·08	102·42	0·78	1·00
	pl	1	58·01	0·09	26·60	0·74	0·00	0·09	9·43	5·29	1·00	101·25	0·17	0·50
25	gl	2	70·73	0·27	16·63	1·72	0·07	0·28	1·92	3·32	3·80	98·77	0·23	0·24
	opx	3	52·59	0·23	1·10	24·57	0·58	19·92	1·82	0·04	0·06	100·90	0·59	0·96
	pl	4	57·49	0·14	25·17	1·38	0·01	0·36	9·33	4·69	1·15	99·73	0·32	0·52
26	gl	3	70·68	0·44	15·81	2·14	0·05	0·47	1·87	3·31	3·71	98·54	0·28	0·24
	opx	4	52·52	0·22	1·21	24·82	0·54	20·02	1·77	0·04	0·09	101·24	0·59	0·96
	pl	2	55·97	0·16	26·63	1·60	0·01	0·18	10·10	4·89	0·88	100·41	0·16	0·53
29	gl	3	69·68	0·36	16·01	1·56	0·09	0·76	2·33	3·01	3·26	97·22	0·47	0·30
	pl	1	55·72	0·11	26·07	1·33	0·03	0·61	10·17	4·98	0·71	99·72	0·45	0·53
30	pl	1	58·33	0·06	25·81	0·57	0·02	0·33	8·33	5·62	1·45	100·52	0·51	0·45
50	gl	7	70·32	0·23	13·34	1·80	0·04	0·32	2·05	3·06	3·14	94·31	0·24	0·27
	hb	4	45·47	1·77	11·58	15·24	0·27	11·77	10·46	1·62	0·57	98·74	0·58	0·78
	pl	5	56·89	0·05	26·35	0·91	0·01	0·16	10·12	4·85	0·35	99·69	0·23	0·54
51	gl	6	74·17	0·19	11·71	1·36	0·02	0·23	1·45	2·72	4·12	95·97	0·23	0·23
	opx	1	52·51	0·18	1·09	26·40	0·65	18·56	1·54	0·00	0·04	100·97	0·56	1·00
	hb	2	46·05	1·87	11·03	16·31	0·25	10·65	9·76	1·60	0·68	98·19	0·54	0·77
	pl	4	58·47	0·21	17·48	7·33	0·17	5·39	6·09	3·23	1·23	99·65	0·57	0·51

range 6–7 wt % H_2O at 300 MPa. Quartz and biotite can also coexist at lower pressure and the combination of our data and those of Venezky & Rutherford (1999) makes it possible to draw a P–T phase diagram at water-saturated conditions (Fig. 6). At water-saturated conditions, quartz and biotite coexist only below 800°C in the range 100–300 MPa. At these conditions ($aH_2O = 1300$ MPa and $T < 800$°C), the crystal fraction in the dacitic composition is *c*. 35 wt % (Table 3). This crystal fraction would be higher if slightly water-undersaturated conditions prevailed.

It has to be emphasized that the investigated composition (bulk dacite) results from a mixing of two magmas. From the model in Fig. 3, the bulk dacite results from the mixing of *c*. 65% of low-temperature magma and 35% of andesitic magma. Thus, the discrepancy between the natural phenocryst mineral assemblage and the experimental phase assemblage (absence of a field with coexisting quartz, biotite, opx, hornblende and plagioclase at post-mixing conditions; 875–900°C and 300 MPa) may be explained by the presence of inherited phenocrysts, which may have only partially re-equilibrated with the post-mixing melt. Although the bulk dacite may not be strictly representative of the low-temperature magma, our results can be applied to constrain, in part, the conditions prevailing in the low-temperature end-member magma prior to mixing. Assuming that the low-temperature magma is composed of at least 35 wt % phenocrysts and at most 65 wt % rhyolitic melt (see above), the bulk composition of this magma must be relatively close to the bulk dacite. Using the phase relations shown in Figs 4 and 6, and assuming a pressure of 300 MPa, it can be concluded that in the low-temperature magma, quartz and biotite can be stable together only at $T < 775$°C. Quartz and biotite were also not stable in experiments with the groundmass composition at 800°C and higher and at 200 and 100 MPa (Sato *et al.*, 1999). Because of this low temperature, the crystallinity of the magma must be high. At 300 MPa and 800°C, the presence of coexisting biotite and quartz in the bulk dacite would be obtained only in magmas containing more than 35% crystals (this crystal fraction would increase at water activity lower than unity and at lower temperature). It should also be noted that the estimated temperature of 775°C, or below, for a biotite- and quartz-bearing low-temperature magma may be

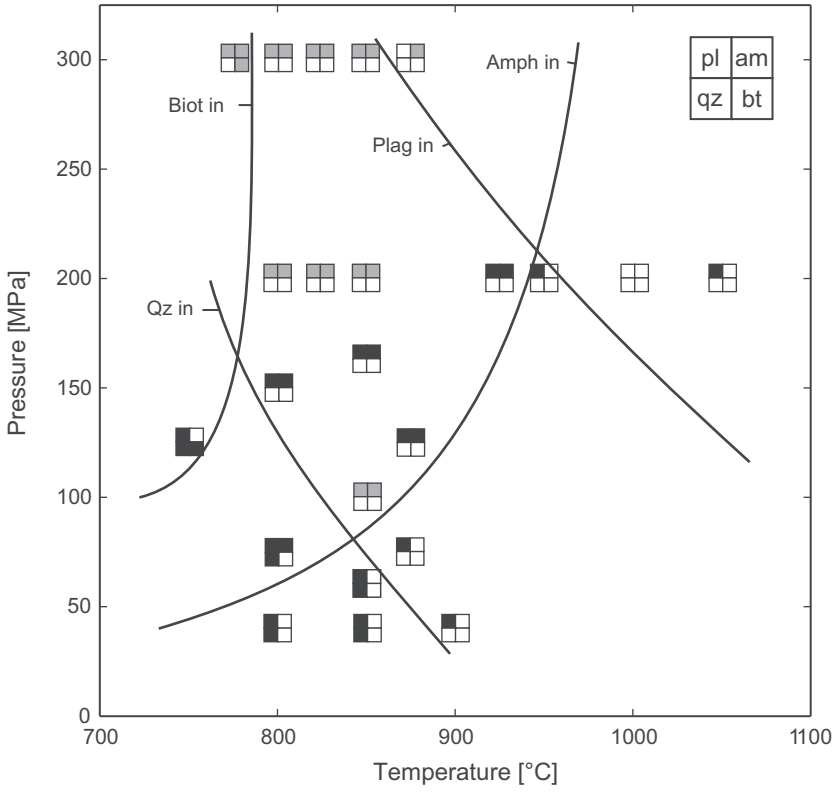

Fig. 6. *P–T* diagram showing the phase relations of the Unzen dacite at water-saturated conditions. For each experiment, the presence of the phases plagioclase, amphibole, quartz and biotite is marked by the grey or black squares: black squares, experiments of Venezky & Rutherford (1999); grey squares, experiments in this study. Two experiments of Venezky & Rutherford (1999) at 120 MPa, 750°C and 200 MPa, 1050°C have not been used to determine the stability fields of amphibole and plagioclase, respectively, as kinetic problems may have occurred in these experiments. The phase diagram shows that quartz and biotite coexist only at temperatures below 800°C at water-saturated conditions in the pressure range 100–300 MPa.

slightly higher if this magma is more SiO_2 rich than the bulk dacite (in this case, the stability of quartz would be shifted to higher temperatures at the same water activity). The constraints on the crystal content of the rhyolitic end-member magma have implications for the viscosity of the Unzen magmas. The crystal content of >35 wt % (~33 vol. %) in the low-temperature magma is greater than the amount of phenocrysts in the Unzen volcanic rocks, estimated to be 23–28 vol. % or below (Nakada & Motomura, 1999). This suggests that only mixed or mingled magmas in which the content of phenocrysts was relatively low were able to migrate towards the surface.

One other possible interpretation for the discrepancy between the natural phenocryst assemblage of the low-temperature end-member magma and the experimental phase assemblage is that phenocrysts may be inherited from different portions of the magma chamber with variations in terms of $X(H_2O)$ and/or temperature. For example, quartz and orthopyroxene phenocrysts could be present in a portion of a magma chamber in which temperature and/or $X(H_2O)$ is lower than in another part of the magma storage system in which phenocrysts such as biotite, hornblende and plagioclase crystallized. This model is consistent with the observation of mutual mineral inclusions in the phenocryst phases. On the other hand, it is known that quartz stability decreases as pressure increases at water-saturated conditions (e.g. Johannes & Holtz, 1996; Barclay *et al.*, 1998; this study). It is, therefore, also possible that part of the phenocryst assemblage was inherited from magma pockets at depths of 5 and 8 km. Although there is a possibility that some low-temperature end-member magma was derived from such shallow magma pockets, we prefer a model in which most of the low-temperature end-member magma was derived from the main magma chamber at a depth of around 11 km. This magma was not necessarily homogeneous in terms of temperature and water activity. In any case, the phase relations show that the crystallinity was high (>35 wt %) and that the water content of the rhyolitic melt was higher than 6 wt % H_2O. Therefore, the low-temperature magma was highly viscous (crystal mush) at the time of injection of the high-temperature magma. In contrast, the viscosity of the rhyolitic residual melt must have been low because of its high water content.

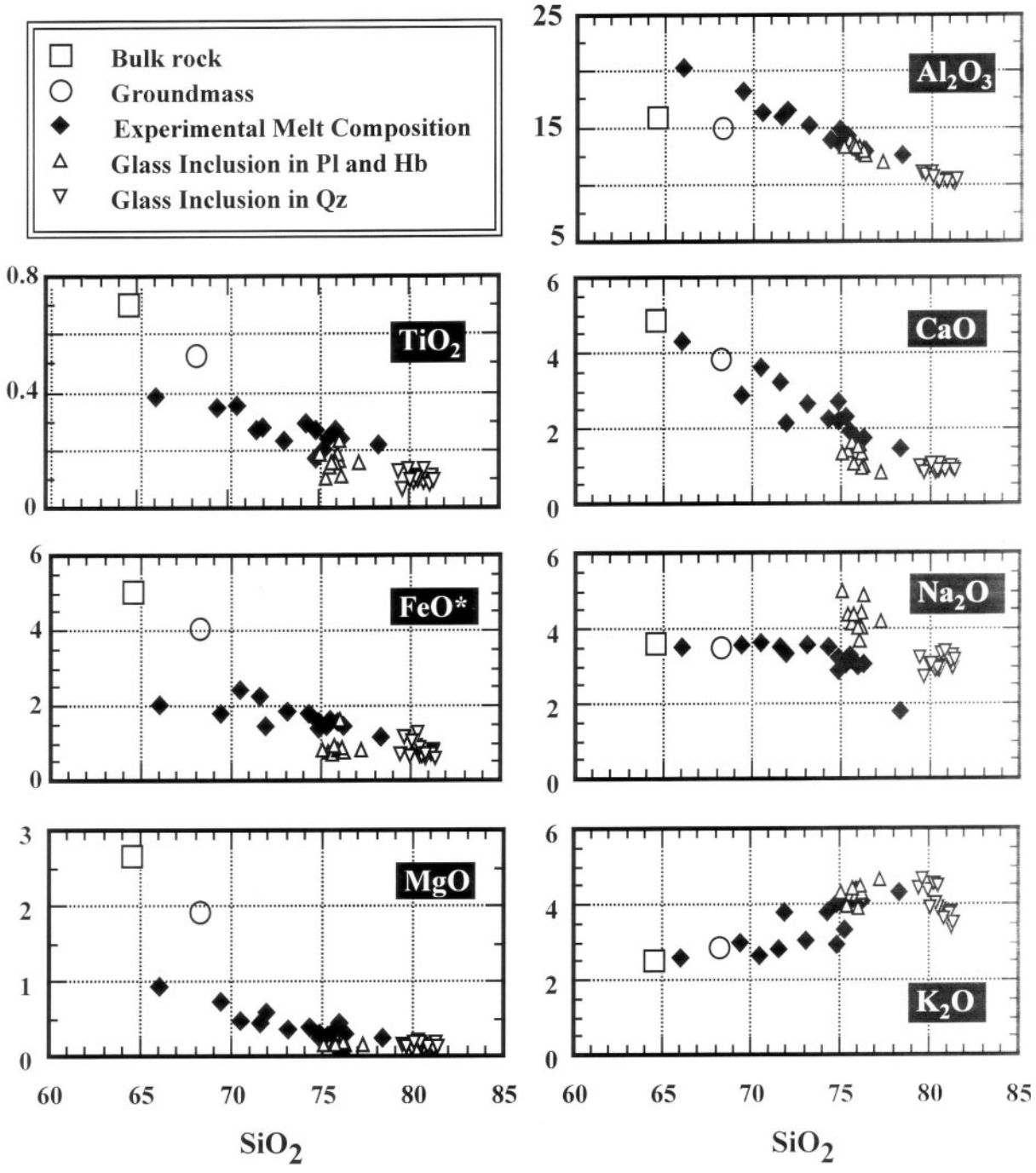

Fig. 7. Variation diagrams showing the compositions of the experimental glasses, glass inclusions in plagioclase, quartz and hornblende, the bulk rock and the groundmass of the Unzen dacite.

Melt and mineral compositions

Figure 7 illustrates the melt compositions of the experimental charges, which are compared with the bulk-rock composition, groundmass composition, and melt inclusions in the phenocrysts. The experimental melt compositions show monotonically varying compositional changes in the oxide–silica diagrams. Although the experimental melt compositions deviate from the natural bulk-rock and groundmass compositions for some elements, such as TiO_2, FeO*, MgO and Al_2O_3, they converge on the melt inclusion compositions with high SiO_2 contents around 75–78 wt %. Glasses with such

high SiO_2 contents have been obtained in runs with high crystal contents.

At low temperature (<800°C; in the stability field of quartz and/or biotite) such high crystal contents are also obtained at high $X(H_2O)$. Thus, glass inclusions in plagioclase may represent the composition of a water-rich rhyolitic liquid resulting from the partial crystallization of a dacitic magma in a magma chamber at depth of 11 km prior to mixing. Experimental glasses with low SiO_2 contents (<70 wt % SiO_2) have FeO*, MgO and TiO_2 contents that differ appreciably from the bulk dacite or groundmass composition (Fig. 7). However, the temperature of the experimental runs was lower than that of the groundmass after mixing, explaining the low Fe, Mg and Ti contents of the experimental glasses when compared with the groundmass composition.

As described in the previous section, plagioclase An contents in the experimental charges range from An_{43} to An_{77}. At temperatures of 775–800°C and $X(H_2O) = 0{\cdot}8–1{\cdot}0$, the An content of plagioclase is $An_{43–52}$, which mostly covers the compositional range of the main population of the plagioclase phenocryst cores (Fig. 1). The minor element concentrations such as MgO, FeO* and K_2O in the experimental plagioclases (MgO >0·1 wt %; FeO* 0·5–1 wt %) are higher than those in the natural plagioclases (Sato, 1996), which may partly result from analytical problems caused by the small grain size of the plagioclases in the experimental run products (Fig. 5), and by kinetic effects of rapid growth of the experimental plagioclases at relatively large undercooling. The most calcic plagioclase phenocrysts in the dacite may have crystallized from more high-temperature magmas. It has to be noted that An-rich compositions are often found between more sodic compositions (oscillatory zoning), and that the calcic plagioclases have low MgO and FeO* contents (Sato, 1996). Thus, we presume that these calcic plagioclases present in the low-temperature end-member magma may record an injection of high-temperature magmas into the low-temperature magma chamber. The complex history of the plagioclase phenocrysts was confirmed by Chen *et al.* (1993, 1999), who compared the $^{87}Sr/^{86}Sr$ isotopic ratios of phenocrysts and matrix of eruptive products of Unzen eruptions of 1991–1995, 1792 and 1663.

The comparison of the Mg-number of natural and experimental mineral phases synthesized at Ni–NiO buffer conditions also allows constraints to be placed on the oxygen fugacity prevailing in the Unzen magma. Hornblendes with Mg-number in the range 0·60–0·66 (observed in the natural rock, Fig. 1) are best reproduced at 825–850°C. The same observation can be confirmed when comparing the population of the natural Fe-rich orthopyroxenes (Mg-number 0·60–0·66, Fig. 1) and the synthetic orthopyroxenes (Mg-number 0·57–0·59). At lower temperature (775°C), the synthesized hornblende and biotite (experiments 11 and 12, Mg-number 0·53–0·55) are slightly more Fe rich than the natural ones. This is also the case when comparing the orthopyroxenes synthesized at 800°C with the natural Fe-rich population. Assuming that a temperature of 775°C or below is representative of the low-temperature magma (see above), the experimental results suggest that the oxygen fugacity in this magma should have been slightly higher than that buffered by the Ni–NiO assemblage [the Mg/(Mg + Fe) value of mafic minerals is known to increase with increasing oxygen fugacity]. This oxygen fugacity is close to that calculated by Nakada & Motomura (1999) and Venezky & Rutherford (1999) for the crystallization of the groundmass, which was found to be 1–2 log units higher than the quartz–fayalite–magnetite buffer. However, experiments at different oxygen fugacities need to be performed to determine exactly the prevailing conditions in the low-temperature magma and in the mixed magma chamber. In addition, there is still very little information on the oxygen fugacity in the high-temperature magma.

CONCLUSIONS

This study provides constraints on the conditions prior to and after the magma mixing event leading to the eruption of the 1991–1995 Unzen dacite. The high-temperature end-member is not completely aphyric with 62–64 wt % SiO_2 at 1055 ± 75°C. The most probable temperature is between 1030 and 1130°C, in agreement with Venezky & Rutherford (1999). The low-temperature end-member magma contains a high fraction of phenocrysts (>35 wt %) and the melt coexisting with the phenocrysts is rhyolitic with a SiO_2 content above 75 wt %. The oxygen fugacity is slightly above that fixed by the Ni–NiO buffer. The temperature of this magma prior to mixing is most probably below 775°C and the water content of the melt is high (at least 6–7 wt % H_2O). Assuming that the water content in the rhyolitic melt prior to mixing is close to the values found in the glass inclusions, it may be as high as 8 ± 1 wt %. Thus, this rhyolitic melt can be considered as a residual melt saturated or nearly saturated with respect to a fluid phase if the main magma chamber is at 300 MPa. In any case, the high water contents found in the rhyolitic inclusions in plagioclases also show that these minerals formed at a pressure of at least 300 MPa (when the glass inclusions were trapped) during part of their history.

The bulk dacite that erupted between 1991 and 1995 at Unzen results from the mixing of *c.* 35 wt % high-temperature magma, 35–40 wt % rhyolitic melt and 25–30 wt % phenocrysts (inherited from the low-temperature magma). It is emphasized that these proportions can only be estimations, as the phenocryst abundance changed by *c.* 5% during the course of the eruption (Nakada & Motomura, 1999). Assuming that

the water content in the rhyolitic melt is *c.* 8 wt %, and that the post-mixing melt contained 5–7 wt % H_2O (conditions required for the stability of the three main minerals plagioclase, amphibole and orthopyroxene at 300 MPa; Fig. 4), the water content of the andesitic melt must have been *c.* 4 wt % (see also model in Fig. 3). This estimation is based on a simple mass balance calculation, involving a mixing of 50% rhyolitic melt with 50% andesitic melt, and is only a rough approximation (melting in the low-temperature magma and crystallization in the high-temperature magma is not taken into account). However, the water contents of melts of both the andesitic and the rhyolitic end-members are significantly higher than estimated previously (Venezky & Rutherford, 1999). Thus, prior to mixing, the viscosities of both melts and their viscosity contrast must have been low ($<10^{5\cdot7}$ Pa s for the rhyolitic end-member, Schulze *et al.*, 1996), which favours an efficient mixing of the mafic and rhyolitic melts.

The complex zoning in plagioclase and amphibole phenocrysts (see also Chen *et al.*, 1993, 1999; Sato *et al.*, 2005) and the difficulty in reproducing the natural phenocryst assemblage (coexistence of biotite, quartz, and orthopyroxene) suggest that the physical conditions of crystallization of these minerals in the low-temperature end-member magma are not necessarily identical throughout the magma body. We suggest that intermittent injection and commingling of high-temperature mafic magmas with the low-temperature phenocryst-rich magma may have occurred. An alternative explanation for the oscillatory zoning of plagioclase and amphibole phenocrysts is that volatile activity changed periodically in the low-temperature magma as a result of the degassing of a deeper high-temperature magma (Sato *et al.*, 2005).

ACKNOWLEDGEMENTS

Thanks are due to W. Johannes, M. Nowak and K. Suzuki-Kamata for discussions during this work. We appreciated the technical assistance of J. Koepke, D. Ziegenbein, O. Diedrich and the technical staff of the workshop at the Institut für Mineralogie at Hannover. I. Kannewischer and M. Freise are thanked for assistance in the preparation of the manuscript. Raman spectroscopic measurements were made at the Institut für Mineralogie at the University of Clausthal–Zellerfeld (Institut für Mineralogie, Professor K. Mengel). Critical comments of J. Barclay and M. Rutherford and the final review of J. Gamble helped to improve the manuscript. This work was supported by the DFG projects Ho1337/7 and Ho1337/11. The collaboration between Kobe and Hannover Universities was initiated by a grant of the JSPS foundation to F.H.

REFERENCES

Barclay, J., Rutherford, M. J., Carroll, M. R., Murphy, M. D., Devine, J. D., Gardner, J. & Sparks, R. S. J. (1998). Experimental phase equilibria constraints on pre-eruptive storage conditions of the Soufrière Hills magma. *Geophysical Research Letters* **25**, 3437–3440.

Blank, J. G., Stolper, E. M. & Carroll, M. R. (1993). Solubility of carbon dioxide and water in rhyolitic melt at 850°C and 750 bars. *Earth and Planetary Science Letters* **119**, 27–36.

Chen, C. H., De Paolo, D. J., Nakada, S. & Shieh, Y.-N. (1993). Relationship between eruption volume and Nd isotopic composition in dacite of Unzen volcano, Japan. *Nature* **362**, 831–834.

Chen, C. H., Nakada, S., Shieh, Y.-N. & De Paolo, D. J. (1999). The Sr, Nd and O isotopic studies of the 1991–1995 eruption at Unzen, Japan. *Journal of Volcanology and Geothermal Research* **89**, 243–253.

Dall'Agnol, R., Scaillet, B. & Pichavant, M. (1999). An experimental study of a lower Proterozoic A-type granite from the eastern Amazonian craton, Brazil. *Journal of Petrology* **40**, 1673–1698.

Devine, J. D., Gardner, J. E., Brack, H. P., Layne, G. D. & Rutherford, M. J. (1995). Comparison of microanalytical methods for estimating H_2O contents of silicic volcanic glasses. *American Mineralogist* **80**, 319–328.

Ebadi, A. & Johannes, W. (1991). Beginning of melting and composition of first melts in the system Qz–Ab–Or–H_2O–CO_2. *Contributions to Mineralogy and Petrology* **106**, 286–295.

Harvie, C., Weare, J. H. & O'Keefe, M. (1980). Permeation of hydrogen through platinum: a re-evaluation of the data of Chou *et al.* *Geochimica et Cosmochimica Acta* **44**, 899–900.

Holtz, F., Behrens, H., Dingwell, D. B. & Johannes, W. (1995). Water solubility in haplogranitic melts. Compositional, pressure and temperature dependence. *American Mineralogist* **80**, 94–108.

Holtz, F., Johannes, W., Tamic, N. & Behrens, H. (2001). Maximum and minimum water contents of granitic melts: a reexamination and implications. *Lithos* **56**, 1–14.

Ishihara, K. (1993). Continuous magma supply inferred from discharge rate of magma and ground deformation rate at Mt. Unzen, Japan. *Annals of the Disaster Prevention Research Institute, Kyoto University* **36**, 219–230 (in Japanese with English abstract).

Johannes, W. & Holtz, F. (1996). *Petrogenesis and Experimental Petrology of Granitic Rocks*. Berlin: Springer, 335 pp.

Johnson, M. C. & Rutherford, M. J. (1989). Experimental calibration of the aluminium-in-hornblende geobarometer with application to Long Valley Caldera (California). *Geology* **17**, 837–841.

Klimm, K., Holtz, F., Johannes, W. & King, P. L. (2003). Fractionation of metaluminous A-type granites: an experimental study of the Wangrah Suite, Lachlan Fold Belt, Australia. *Precambrian Research* **124**, 327–341.

Lindsley, D. H. & Frost, B. R. (1992). Equilibria among Fe–Ti oxides, pyroxenes, olivine and quartz: Part I. Theory. *American Mineralogist* **77**, 987–1003.

Luhr, J. F. (1990). Experimental phase relations of water- and sulfur-saturated arc magmas and the 1982 eruptions of El Chichón volcano. *Journal of Petrology* **31**, 1071–1114.

Martel, C., Pichavant, M., Holtz, F., Scaillet, B., Bourdier, J.-L. & Traineau, H. (1999). Effects of fO_2 and H_2O on andesite phase relations between 2 and 4 kbar. *Journal of Geophysical Research* **104**, 29453–29470.

Nakada, S. & Fujii, T. (1993). Preliminary report on the activity at Unzen volcano (Japan), November 1990–November 1991: dacite lava domes and pyroclastic flows. *Journal of Volcanology and Geothermal Research* **54**, 319–333.

Nakada, S. & Motomura, Y. (1999). Petrology of the 1991–95 eruption at Unzen: effusion pulsation and groundmass crystallization. *Journal of Volcanology and Geothermal Research* **89**, 173–196.

Nakamura, M. (1995). Continuous mixing of crystal mush and replenished magma in the ongoing Unzen eruption. *Geology* **23**, 807–810.

Nakamura, M. (1996). Time scale of magma mixing in Unzen eruption from 1991 to 1993: continuous mixing model of crystal-rich magma and replenished magmas. *Memoirs of the Geological Society of Japan* **46**, 127–138.

Nishi, K., Ono, H. & Mori, H. (1999). Global positioning system measurements of ground deformation caused by magma intrusion and lava discharge: the 1990–1995 eruption at Unzendake volcano, Kyushu, Japan. *Journal of Volcanology and Geothermal Research* **89**, 23–54.

Rutherford, M. J., Sigurdsson, H. & Carey, S. (1985). The May 18, 1980 eruption of Mount St. Helens: I, Melt composition and experimental phase equilibria. *Journal of Geophysical Research* **90**, 2929–2947.

Sato, H. (1996). A model of the 1991 eruption of Unzen volcano inferred from petrographic textures of the ejecta. *Memoirs of the Geological Society of Japan* **46**, 115–125.

Sato, H., Nakada, S., Fujii, T., Nakamura, M. & Suzuki-Kamata, K. (1999). Groundmass pargasite in the 1991–1995 dacite of Unzen volcano: phase stability experiments and volcanological implications. *Journal of Volcanology and Geothermal Research* **89**, 197–212.

Sato, H., Holtz, F., Behrens, H., Botcharnikov, R. & Nakada, S. (2005). Experimental petrology of the 1991–1995 Unzen dacite, Japan. Part II: Cl/OH partitioning between hornblende and melt and its implications for the origin of oscillatory zoning of hornblende phenocrysts. *Journal of Petrology* **46**, 000–000.

Satoh, H., Saito, G., Shinohara, H. & Yamaguchi, Y. (2003). Sulfur source for the 1991–1995 Unzen eruption: evidence from melt inclusions in pyroxenes. *Geophysical Research Letters* **30**, 2220.

Scaillet, B. & Evans, B. W. (1999). The 15 June 1991 eruption of Mount Pinatubo. I. Phase equilibria and pre-eruption P–T–fO$_2$–fH$_2$O conditions of the dacite magma. *Journal of Petrology* **40**, 381–411.

Schmidt, M. W. (1992). Amphibole composition in tonalite as a function of pressure: an experimental study at 650°C. *Contributions to Mineralogy and Petrology* **110**, 304–310.

Schulze, F., Behrens, H., Holtz, F., Roux, J. & Johannes, W. (1996). The influence of water on the viscosity of a haplogranitic liquid. *American Mineralogist* **81**, 1155–1165.

Sparks, R. S. J. & Marshall, L. A. (1986). Thermal and mechanical constraints on mixing between mafic and silicic magmas. *Journal of Volcanology and Geothermal Research* **29**, 99–124.

Sugawara, T. (1998). Thermodynamic analysis of Fe and Mg partitioning between plagioclase and silicate liquid. *Contributions to Mineralogy and Petrology* **138**, 101–113.

Tamic, N., Behrens, H. & Holtz, F. (2001). The solubility of H$_2$O and CO$_2$ in rhyolitic melts in equilibrium with a mixed CO$_2$–H$_2$O fluid phase. *Chemical Geology* **174**, 333–347.

Thomas, R. (2000). Determination of water contents of granite melt inclusions by confocal laser Raman microprobe spectroscopy. *American Mineralogist* **85**, 868–872.

Venezky, D. Y. & Rutherford, M. J. (1999). Petrology and FeTi oxide reequilibration of the 1991 Mount Unzen mixed magma. *Journal of Volcanology and Geothermal Research* **89**, 212–230.

Webster, J. D., Kinzler, R. J. & Mathez, E. A. (1999). Chloride and water solubility in basalt and andesite melts and implications for magmatic degassing. *Geochimica et Cosmochimica Acta* **63**, 729–738.

Yamaguchi, Y. (1997). Chlorine, sulfur and fluorine contents of melt inclusions in phenocrysts, matrix glass, and cryptocrystalline phases in dacites of the 1991 eruption, Unzen volcano. In: Nakada, S. (ed.) *Proceedings of the 1997 Unzen Workshop*, Tokyo: Earthquake Research Institute, pp. 117–119.